The Canadian Mineralogist
Vol. 43, pp. 1141-1156 (2005)

GEOCHEMICAL AND MINERALOGICAL ZONING OF HIGH-SULFIDE MINE-WASTE AT THE BERIKUL MINE-SITE, KEMEROVO REGION, RUSSIA

NIKOLAY V. SIDENKO[§], ELENA V. LAZAREVA, SVETLANA B. BORTNIKOVA AND ALBERT D. KIREEV

Institute of Geology, Siberian Branch, Russian Academy of Sciences, pr. ac. Koptyuga 3, Novosibirsk 630090, Russia

BARBARA L. SHERRIFF

Department of Geological Sciences, University of Manitoba, Winnipeg, Manitoba R3T 2N2, Canada

ABSTRACT

Geochemical zoning of the high-sulfide (40–45 wt.% sulfides) and low-carbonate (3 wt.% dolomite) waste at the Berikul gold mine, Kemerovo region, Russia, was studied in order to understand the processes controlling As, Cd, Cu , Pb and Zn migration from the waste. The following zones were distinguished from bottom to top: (1) slightly altered waste, (2) cemented hardpan zone, (3) melanterite zone, (4) intermediate zone and (5) jarosite zone. A sequential scheme of extraction was used to separate (a) water-soluble, (b) exchangeable, (c) carbonate, (d) phases bound with Fe^{3+}, and (e) residual fractions of Fe, As, Zn, Cu and Cd. The two basal zones reflect an early stage of weathering, where acid generated by sulfide oxidation is neutralized by carbonate. Neutralization processes promote coprecipitation of As, Cd, Cu, Pb and Zn in Fe^{3+} phases, such as amorphous Fe sulfo-arsenate and jarosite. An intermediate stage, recorded in the melanterite and intermediate zones, is identified by the disappearance of the carbonates and a decrease in the pH of pore solutions. At low pH, sulfides are oxidized by Fe^{3+}, producing Fe^{2+}, SO_4^{2-}, and liberating As, Zn, Cu and Cd, which accumulate in the pore water. This step results in the precipitation of Zn-, Cu- and Cd-bearing melanterite. The intermediate stage of weathering continues until most of the sulfide fraction has been oxidized. Then, as shown in the upper jarosite zone, the concentration of Fe^{3+} again increases in the pore waters because it is not being utilized in sulfide oxidation, and Fe^{3+} phases, such as jarosite, precipitate. By this stage, significant amounts of As, Zn, Cu and Cd have been leached from the weathered residue, but Pb precipitates in the jarosite.

Keywords: arsenic, zinc, copper, lead, mine waste, sulfide oxidation, sequential extraction, melanterite, jarosite, Berikul gold mine, Kemerovo region, Russia.

SOMMAIRE

Nous avons étudié la zonation géochimique des déchets à concentration élevée de sulfures (40–45%, poids) et à faible teneur en carbonate (3%) de la mine d'or de Berikul, région de Kemerovo, en Russie, afin de mieux comprendre les processus régissant la migration de As, Cd, Cu , Pb et Zn à partir des déchets. On distingue les zones suivantes du bas vers le haut: (1) déchets légèrement altérés, (2) zone durcie et cimentée, (3) zone à mélanterite, (4) zone intermédiaire, et (5) zone à jarosite. Un schéma d'extraction séquentielle a été utilisé pour séparer (a) composants solubles dans l'eau, (b) composants échangeables, (c) fraction carbonatée, (d) phases liées au Fe^{3+}, et (e) fractions résiduelles de Fe, As, Zn, Cu et Cd. Les deux zones à la base résultent d'un stade précoce de lessivage, dans lequel l'acide généré par l'oxydation de sulfures est neutralisé par le carbonate. Les processus de neutralisation favorisent la coprécipitation de As, Cd, Cu, Pb et Zn dans des phases riches en Fe^{3+}, par exemple une phase amorphe sulfo-arsenatée de fer et la jarosite. Un stade intermédiaire, enregistré dans les zones à mélantérite et intermédiaire, est identifié par la disparition de carbonates et une diminution du pH des solutions interstitielles. A faible pH, les sulfures sont oxydés par le Fe^{3+}, produisant Fe^{2+}, SO_4^{2-}, et libérant As, Zn, Cu et Cd, qui s'accumulent dans les solutions interstitielles. Cette étape mène à la précipitation de mélantérite contenant Zn, Cu et Cd. Le stade intermédiaire du lessivage continue jusqu'au point où la plupart de la fraction sulfurée a été oxydée. A ce point, comme le démontre la zone supérieure à jarosite, la concentration du Fe^{3+} augmente de nouveau dans les solutions interstitielles parce qu'il n'est plus utilisé dans l'oxydation des sulfures, et les phases riches en Fe^{3+} se forment, comme la jarosite. A ce point, des quantités importantes de As, Zn, Cu et Cd sont mobilisées du résidu lessivé, mais le Pb est accommodé dans la jarosite.

(Traduit par la Rédaction)

Mots-clés: arsenic, zinc, cuivre, plomb, déchets miniers, oxydation de sulfures, extraction séquentielle, mélantérite, jarosite, mine d'or de Berikul, région de Kemerovo, Russie.

§ *E-mail address*: sidenkon@cc.umanitoba.ca

Introduction

Where sulfidic mine-tailings are exposed to oxygen and water, they can generate acidic solutions containing high concentrations of base metals, which are potential ecotoxicants. Metal leaching and acid generation depend on the reactivity of sulfides, which varies with the conditions of weathering (Jambor 1994). Geochemical zoning in sulfidic mine-wastes has been studied widely and used to describe the chemical reactions controlling the acidity and concentrations of elements in pore water (Blowes & Jambor 1990, Blowes *et al.* 1991, Blowes & Ptacek 1994). If carbonate is present in the tailings, the acidity in the lower zones is buffered by dissolution of carbonate minerals, resulting in coprecipitation of metals in secondary phases, such as Fe hydroxides. In the upper carbonate-depleted zones, pH decreases, and metals may be released back into pore water by the dissolution of secondary phases (Blowes & Ptacek 1994). Further migration of the ecotoxicants might cause surface and groundwater pollution. This study was initiated because discharge of acidic solutions draining from the mine wastes into the Mokry Berikul River, in Russia, will continue to cause damage the phyto- and zooplankton populations (Bortnikova *et al.* 2001) unless remedial action is taken.

Background Information

The Berikul gold mine is situated in the northern part of the Kemerovo region, in western Siberia, about 450 km northeast of Novosibirsk (Fig. 1). The ore deposit consists of quartz–sulfide veins at the contact of dolomitic limestone and diorite. Fine-grained gold, which is intergrown with pyrite and arsenopyrite, was extracted at the Berikul mill by sulfide flotation and subsequent cyanidation of the sulfide concentrate. After the removal of the gold-bearing cyanide solutions, the sulfide residues were transported by trucks and dumped as a waste pile on alluvial carbonate boulders on the north bank of the Mokry Berikul River (Fig. 2). The waste pile is about 250 m in length, and 50 m wide at the base, with a height of 3–5 m. Discharged material is composed of 40–45 wt.% fine-grained sulfides (less than 50 μm), pyrite (35–40 wt.%), arsenopyrite (2–5 wt.%), and minor amounts of pyrrhotite, sphalerite, chalcopyrite, galena, quartz, albite, chlorite, muscovite, and dolomite. This waste material has been in existence since 1952.

Our previous studies focused on the impact of the river pollution on aquatic life, porewater and surface-water composition, and on the mineralogical control of water composition (Bortnikova *et al.* 2001, Sidenko 2001, Sidenko *et al.* 2001, Gieré *et al.* 2003). A previous mineralogical and hydrogeochemical study showed the Berikul mine waste to generate acidic drainage (pH about 1.1), which contains very high concentrations of SO_4^{2-}, Fe, Zn and As (Gieré *et al.* 2003). Within the pile, As and Pb were precipitated as amorphous non-stoichiometric ferric sulfo-arsenates and jarosite–beudantite solid solutions, which are relatively insoluble (Sidenko *et al.* 2001, Gieré *et al.* 2003). Transition metals, such as Cu and Zn, accumulated in the soluble Fe sulfate minerals such as melanterite, rozenite, copiapite and

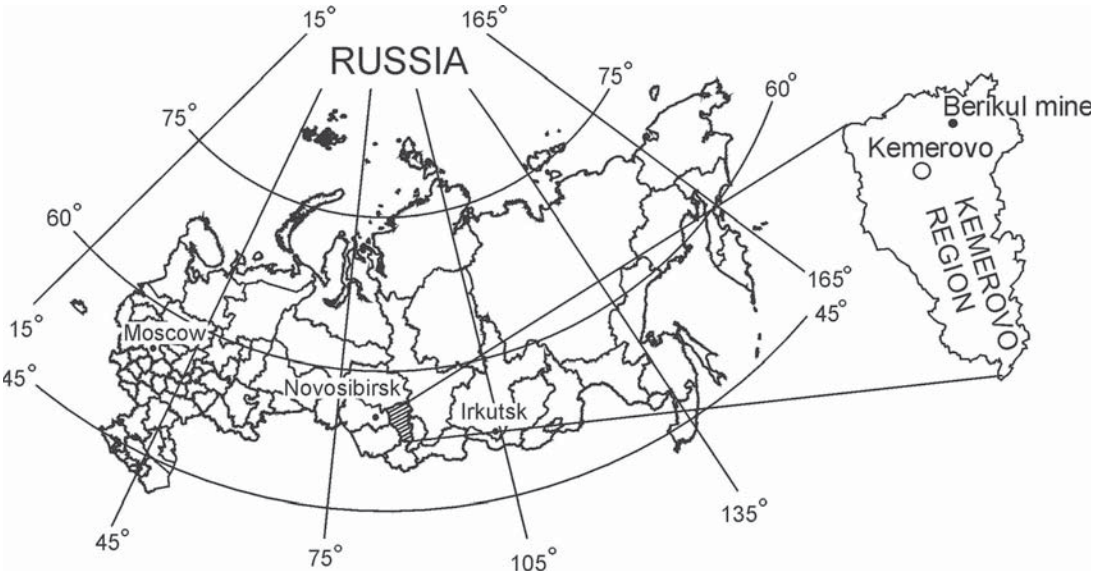

FIG. 1. Map showing the location of the Berikul gold mine, in the Kemerovo region of southwestern Siberia, Russia.

rhomboclase. The last three of these minerals precipitate as efflorescent crusts on the slopes of the pile and are subject to dissolution in periods of rain. The dissolution of the sulfates results in the release of metals into the Mokry Berikul River. This process is the final step in the migration of elements from the mine waste to the aquatic biota.

The initial processes determining the release of metals from sulfides and the conditions controlling the geochemistry within the waste pile were not previously studied, and details about the formation of secondary Fe-phases were not explained. For example, the reasons for the existence of a thick layer of melanterite between zones comprised of Fe^{3+} phases (*e.g.*, jarosite) were not known (Gieré *et al.* 2003). Thus, this geochemical study was initiated to fill the gaps in our understanding of the processes that control the redistribution of As, Zn, Cu, Cd, and Pb within the high-sulfide mine wastes. Our first task was to quantify the distribution of Fe, As, Zn, Cu, Cd and Pb in primary sulfides and in different secondary phases. The second task was to distinguish individual buffering reactions in each zone in order to understand better their effect on the stability of the secondary phases.

Methodology

Sampling

Representative samples were collected from the exposed walls of pits 3 m deep dug into the waste pile (Fig. 2). Samples were hermetically sealed in polyethylene bags and frozen immediately to preserve the *in situ* chemical characteristics of pore waters.

Analytical techniques

In the laboratory, the samples were thawed, and pore solutions squeezed from the moist silty material at a pressure of 100 Pa. No water could be extracted from dry or cemented "hardpan" layers. The techniques and results of water analyses were reported previously (Sidenko *et al.* 2001, Gieré *et al.* 2003). After the pore water had been removed, an aliquot of the solid sample was dried at room temperature for one week and powdered using an agate mortar and pestle to about 0.05 mm. Polished sections were prepared from an uncrushed aliquot of the samples.

Polished sections were studied by reflected light microscopy and scanning electron microscopy (JEOL JSM–36) to compare the relative degree of alteration of various sulfide minerals. Interpretations of the geochemical results of this study are based on previous mineralogical data, which have been obtained using X-ray powder diffraction, thermogravimetric analysis, and electron-microprobe analysis (Gieré *et al.* 2003).

The contents of CO_2, S_{total} and $S_{sulfate}$ were determined by gravimetric techniques. Carbonates were dissolved in 6N HCl, with the evolved CO_2 being passed through an Ascarite® mixture, in which the carbonates were precipitated as Na_2CO_3. Total S was measured using the gravimetric method described by Jeffery & Hutchison (1983). Sulfate S was determined as the difference between S_{total} and sulfur remaining

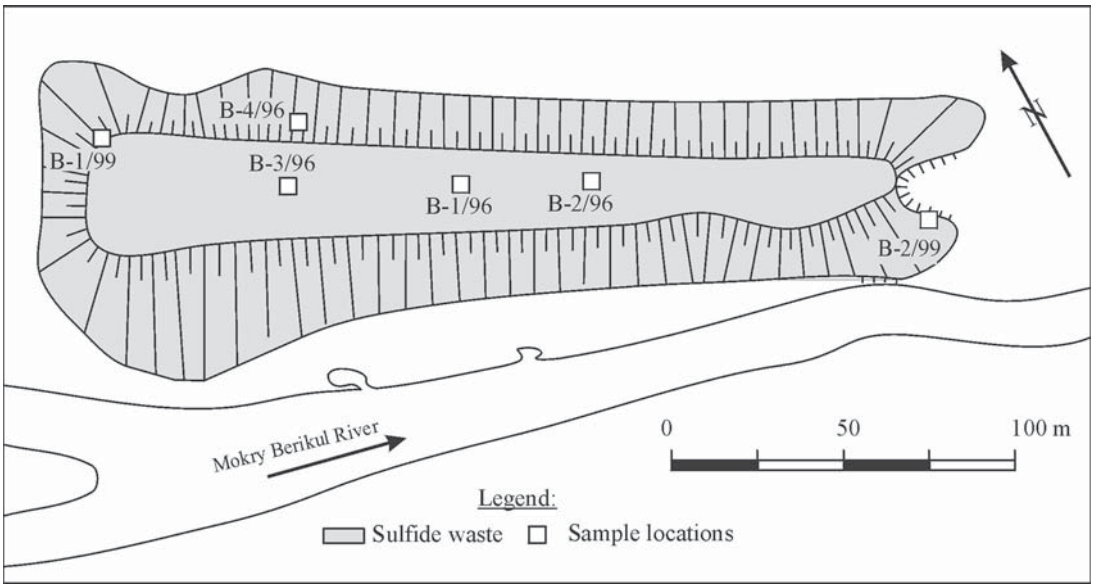

FIG. 2. Sample locations at the Berikul site, modified from Gieré *et al.* (2003).

in the samples after leaching with hot 5 wt.% Na_2CO_3 aqueous solution. Detection limits were 0.44 wt.% for CO_2, and 0.2 wt.% for all S species.

A sequential extraction procedure was used to determine the form of Fe, As, Zn, Cu, Pb and Cd in a set of representative samples. The technique was developed by Tessier *et al*. (1979) for lake sediments. Various modifications of the technique have been later applied to mine tailings (McGregor *et al*. 1995, Ribet *et al*. 1995, Fanfani *et al*. 1997, Dold & Fontboté 2001). We used the original technique of Tessier *et al*. (1979), but the extractions of reducible fractions were optimized to dissolve ferric sulfo-arsenates. This sequence was followed using 1 g of sample in a centrifuge tube. After each step of extraction (a–d), the solid residue was separated from the soluble fraction by centrifuging at 10,000 rpm for 10 minutes and rinsed with 5 mL of distilled water.

a) Water-soluble fractions were extracted by agitation with 20 mL distilled water for 30 minutes at room temperature. Preliminary drying of the samples should affect the stability of soluble hydrates such as melanterite by dehydration and oxidation of Fe^{2+}. We had found previously that melanterite could be transformed into rozenite, and finally, into copiapite (Sidenko *et al*. 2001), but as these are also soluble sulfates of Fe, the drying process should not have any effect on the extraction of soluble Fe and the metals captured by melanterite.

b) Exchangeable and sorbed metals were leached with 15 mL of 1 M $MgCl_2$ solution for 1 hour.

c) The carbonate fraction was extracted by dissolution in 15 mL of 1 M CH_3COONa solution for 5 hours at room temperature. The pH was buffered at 5 with acetic acid.

d) The reducible fraction containing elements bound with ferric Fe phases was extracted by 30 mL of 2 M NH_2OH•HCl solution in 25 vol.% acetic acid at <96ºC for 6 hours. The concentration of NH_2OH•HCl and the time for complete extraction were experimentally derived to dissolve iron sulfo-arsenates completely without a significant attack on the arsenopyrite (see below).

e) The residual sulfides and silicates were dissolved using the HF–HNO_3–$HClO_4$ digestion technique (Bock 1984).

Concentrations of elements were determined by atomic absorption spectroscopy (AAS) using a Perkin–Elmer spectrometer, model 3030E equipped with an HGA–600 graphite furnace. The following standards were used: KS–1 and GSO7330–96 for Cd, Cu, Fe, Pb, Zn, and GSO7264–96 for As. The reproducibility from the triplicate aliquots of eight samples was found to be within 37% for As, 22% for Cd, 15% for Cu, 12% for Fe, 35% for Pb, and 12% for Zn of total concentration of the elements. The low reproducibility was probably caused by a summation of errors produced during each step of the extraction. Fractions of the elements determined by sequential extraction are operationally defined (*i.e.,* selectivity depends on such factors as the time of contact, the solid-to-liquid ratio, and the grain size, which can vary among samples). The average content of elements in each cross-section was weighted according to the thickness of the sampling interval (Table 1).

Prior to the sequential extractions, optimal leaching parameters for the dissolution of amorphous Fe sulfo-arsenates were determined experimentally, because the selectivity of NH_2OH•HCl in 25 vol.% acetic acid with respect to these poorly studied phases was not known. Also, the proportion of As that could be leached from sulfides during this dissolution was determined. Single crystals of arsenopyrite, pyrite, and quartz were obtained from the Geological Museum of the Institute of Geology, Siberian Branch of the Russian Academy of Sciences. Two mixtures were prepared containing mineral phases in similar proportions to those in the samples of waste; the first contained 10 wt.% of amorphous Fe sulfo-arsenates hand-picked from the Berikul samples, and 90 wt.% of quartz sand, and the second contained 10 wt.% arsenopyrite, 30 wt.% pyrite and 60 wt.% quartz. Both mixtures were finely ground. The two mixtures contained similar contents of As, 1.39

TABLE 1. CHEMICAL COMPOSITIONS AND NET NEUTRALIZING POTENTIAL OF SAMPLES FROM SECTIONS B-2/99 AND B-1/96

Zone	Sample	Depth	h	CO_2^{2-}	$S_{sulfide}$	S_{total}	NNP*
				Section B-2/99			
5	B-2/1	5	20	<0.44	<0.2	20.0	0
	B-2/2	23	5	<0.44	11.2	25.8	-349
4	B-2/3	30	15	0.44	15.0	30.4	-459
3a	B-2/4	45	60	0.44	12.7	30.5	-386
	B-2/5	75	20	<0.44	18.0	30.5	-561
	B-2/6	125	30	<0.44	6.3	24.6	-169
2	B-2/7	155	40	<0.44	13.5	26.0	-421
	B-2/8	180	20	0.88	16.8	25.2	-507
1	B-2/9	210	40	0.66	21.6	27.6	-661
	B-2/10	275	50	1.98	21.6	24.7	-636
				Section B-1/96			
5	BK-1	2.5	5	<0.44	<0.2	5.2	0
	BK-2	10	10	<0.44	<0.2	5.2	0
4	BK-4	25	15	<0.44	2.6	10.2	-81
	BK-5	40	15	<0.44	12.6	16.8	-393
3b	BK-6	60	10	12.8	3.1	4.3	152
	BK-8	70	15	12.5	3.6	5.4	131
2	BK-9	80	15	0.9	13.9	16.8	-416
	BK-10	95	15	3.7	6.3	10.2	-122

Note: depth: shows the center of the sampled interval in cm, h: thickness of sampled interval in cm. Zone names: 1: *slightly altered sulfide waste*, 2: *hardpan layer*, 3a: *melanterite zone*, 3b: *carbonate lens*, 4: *intermediate zone*, 5: *jarosite zone*.
* NNP: net neutralizing potential (kg $CaCO_3$) as determined from the chemical analysis of S and CO_2 assuming that the only carbonate is dolomite (Paktunc 2003). The chemical constituents are reported in wt.%.

and 1.43 wt.%, respectively. The parameters for the extraction of the reducible fraction were varied to find the optimal time of leaching and the concentration of As in the leachate. The concentration of NH_2OH•HCl at 25 vol.% acetic acid was varied from 0.04 to 2 M. Aliquots of 2 mL were collected after 1, 3, 6 and 8 hours of dissolution, and the concentrations of As and Fe were determined by AAS. The optimal condition for As extraction (*i.e*., 99.4 % of total As) was found to be with 2 M NH_2OH•HCl solution for 6 hours (Fig. 3). Under these conditions, 9.3 wt % of As was leached from the arsenopyrite in the sulfide mixture. Thus, it is possible that the reported As values in the reducible fraction are overestimated by as high as 10%. About 85% of total Fe was extracted from the first mixture, and 6.3% from the second one under these conditions. According to this, Fe values were systematically underestimated by about 10%.

Stratigraphy and Lithology

Zones at sampling sites were distinguished by color, degree of lithification, relative moisture content, and mineral composition (Gieré *et al*. 2003). Zoning patterns in different sections vary slightly, but the sequences of the layers are similar (Fig. 4). The zones of section B–2/99 are described in detail, because the section is more complete than the others. Five main zones (names given in italics) can be distinguished from bottom to top. Details about the alteration of sulfide grains were added to the description of the zones previously published (Sidenko *et al*. 2001, Gieré *et al*. 2003).

Zone 1 is 1–3 m thick, and extends from the base of the pile to 2 m below the surface. It consists of friable, gray-green, *slightly altered sulfide waste*. During sampling, the material disintegrated into 1–2 cm pieces, indicating that some lithification of initially fine-grained waste had occurred, even at this shallow depth. The beginning of sulfide oxidation is shown by Fe hydroxides replacing pyrrhotite and a rim of alteration products forming around galena, although pyrite and arsenopyrite grains remain angular and unaltered (Figs. 5a, b). Secondary phases include gypsum and reddish films of X-ray-amorphous ferric sulfo-arsenates with variable chemical compositions. Three groups of amorphous Fe sulfo-arsenates were distinguished on the basis of their composition and visual properties (Sidenko *et al*. 2001, Gieré *et al*. 2003). Material of this zone is interpreted to be *slightly altered sulfide waste*. It is the least weathered and closest to the original composition of all observed zones. Therefore, this zone is used as a standard for comparison of geochemical characteristics.

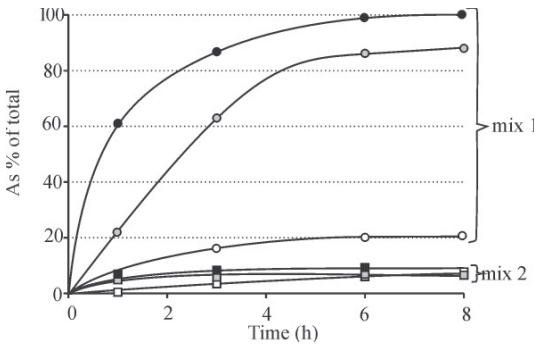

FIG. 3. The effect of NH_2OH•HCl concentration (0.04 M white, 1 M grey, and 2 M black symbols) on As extraction from mixture #1 (circles), 10% amorphous iron sulfo-arsenates and 90% quartz; mixture #2 (squares), 10% arsenopyrite, 30% pyrite and 60% quartz.

Zone 2 is a gray *hardpan layer,* about 1 m thick, that overlies the *slightly altered sulfide waste* of Zone 1. As this layer was very difficult to penetrate, three of the pits were excavated just to this depth. The zone contains cavities, indicating that leaching processes have occurred. Significant replacement of pyrrhotite and galena (Figs. 6a, b) as well as corrosion of arsenopyrite, were observed in close proximity to the leached cavities, but the sulfides in general look similar to those in *slightly altered waste*. Close to the cavities, the grain size of pyrite and arsenopyrite decreases from 50 to 30 μm. Gypsum grains 0.3–1 mm in size form the "skeleton" or "framework" of the *hardpan layer* (Gieré *et al*. 2003). The cavities are filled with jarosite and amorphous Fe sulfo-arsenates. The lithified material is dry, but droplets of a red solution and moist, gel-like mixtures of amorphous Fe sulfo-arsenates were observed on the wall of the cavities.

Zone 3a covers the *hardpan* layer; it is 1.1 m thick and comprised of *melanterite* aggregates up to 10 cm across, and leached relics of hardpan which, in some cases, are overgrown by melanterite. Space between these relics and the melanterite aggregates is filled by water-saturated silty material (Fig. 4). The zone consists of about 25% melanterite, 55% silt and 20% hardpan relics by volume. The presence of the hardpan relics in the horizon above the actual *hardpan layer* indicates that the lithified waste is slowly dissolving during weathering, although there is no significant difference in the degree of alteration and grain size of sulfide grains between zones 2 and 3a.

Zone 4, the *intermediate zone,* 0.1 to 0.5 m thick, separates the *melanterite zone* from the overlying *jarosite zone*. This gray zone gradually changes upward to a yellow color, producing a diffuse boundary with the uppermost zones. Material of the *intermediate zone* is loose, consisting of quartz, jarosite, sulfides and gypsum. A thin alteration-induced rim (<1 μm) surrounds pyrite, chalcopyrite and sphalerite, but arsenopyrite seems more altered compared to these sulfides (Figs. 6c, d, e). Galena and pyrrhotite were not found in this zone. The moisture content of this layer is lower

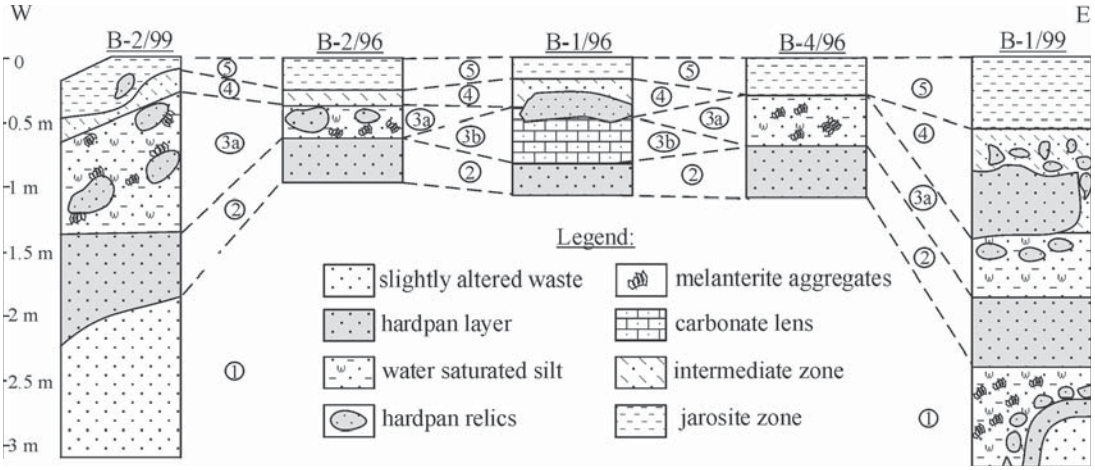

FIG. 4. Correlation scheme of zones from different sections of the Berikul mine-waste. Name of the zones: 1: *slightly altered sulfide waste*, 2: *hardpan layer*, 3a: *melanterite zone*, 3b: *carbonate lens*, 4: *intermediate zone*, 5: *jarosite zone*.

than that of the underlying zone, whereas the grain size is similar at about 20–30 μm.

Zone 5 is the uppermost bright yellow *jarosite zone*, is up to 0.5 m thick; it contains some strongly oxidized relics of hardpan material. The predominant phases are jarosite, quartz and gypsum, with minor pyrite and chalcopyrite (Fig. 5d), which seem to be the most stable sulfides. The grain size of the sulfides is about 20 μm.

The sequences of the zones exposed in sections B–2/96 and B–4/96 are similar to B–2/99, but individual zones are narrower because these sections are located in the center of the pile (Fig. 2), where weathering processes may have been slower than those occurring near the edge. Also, hardpan relics were not found in section B–4/96.

In section B–1/96, a loose lens consisting of gangue minerals with about 10% dolomite was found instead of the melanterite zone. This material is dry, a reddish color and overlain by relics of *hardpan*. The lens may be the result of the occasional discharge of flotation waste consisting of gangue minerals. This zone is referred to as zone 3b, or carbonate lens (Fig. 4).

In section B–1/99, zones 2–5 resembles those in B–2/99 with the exception that melanterite was not found in zone 3a. The complex sequence in the section B–1/99 may reflect the presence of initial heterogeneity of the layers resulting in a complexity of the weathering profile.

Samples from sections B–2/99 and B–1/96 were selected for a detailed geochemical study because B–2/99 represents the general pattern of zonation and B–1/96 contains a possible barrier owing to the presence of carbonate.

GEOCHEMICAL ZONING

Concentrations of sulfur and carbonate

The distribution of sulfur species and CO_2 over the cross-sections reflects the original distribution of minerals, the processes of sulfide oxidation, and acid neutralization by carbonate dissolution (Table 1). The highest sulfide sulfur content (21.6 wt. %) was observed in *slightly altered waste* at the base of section B–2/99 (B–2/9, B–2/10). In general, values of sulfide sulfur decrease from the base of the pile to the surface (Fig. 7), with values being below the detection limit (*i.e.*, <0.2 wt.%) in the uppermost *jarosite zone,* indicating increased oxidation of sulfides upward. The trend for sulfate is opposite to the distribution of sulfide sulfur, with low values being found at the base of the cross-sections, and high values at the top (Fig. 7).

The maximum concentrations of CO_2 were found in samples BK–8 and BK–6 from the carbonate lens in section B–1/96. In section B–2/99, concentrations of CO_2 are about 2% in the basal layer (sample B–2/10) and below the detection limit at the boundary of the *hardpan* and *melanterite zones*, indicating the level of complete dissolution of carbonate. After the dissolution of dolomite, Mg can precipitate as hydrated sulfates, such as epsomite and hexahydrite. However, these minerals were not observed, although the pore waters are supersaturated with respect to epsomite (Sidenko *et al.* 2001). Magnesium might also accumulate in melanterite, which is capable of incorporating up to 50% Mg (Jambor *et al.* 2000).

The net neutralizing potential (NNP) was calculated from sulfide and carbonate content using the mNP

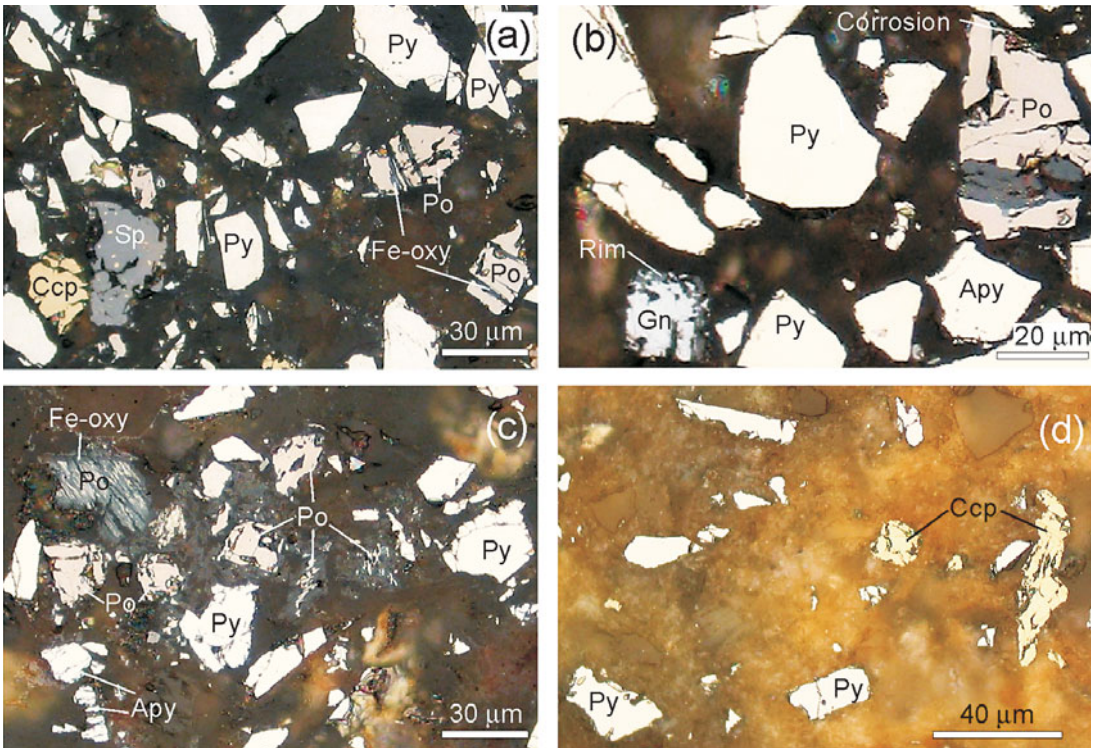

FIG. 5. Photomicrographs of polished sections showing differing degrees of alteration of pyrite (Py), pyrrhotite (Po), chalcopyrite (Ccp), sphalerite (Sp), and galena (Gn) in samples B–2/10 (a, b), B–2/8 (c), and B–2/1 (d).

computer program, assuming Fe-free dolomite to be the dominant carbonate (Table 1, Paktunc 2003). Average value of NNP are –444 and –117 kg/$CaCO_3$ eq/t for sections B–2/99 and B–1/96, respectively. Negative values suggest the potential for acid production.

Concentrations of Fe, As, Zn, Cu, Cd, and Pb

The vertical distribution of the elements (Fig. 8) may reflect an initial heterogeneity of the waste pile owing to changes in the initial composition of the wastes and to post-depositional alteration. There is no documentation regarding changes in initial mineralogy of the tailings, but alteration of the top portion has been described (Gieré *et al*. 2003).

The concentration of total Fe ranges from 5.0 to 28.7 wt.% (Table 2, Fig. 8). High values were found in the *slightly altered sulfide waste* (27.8 wt.% in section B–2/99, and 16.4% in section B–1/96) and *in sulfide relics* (28.7 wt.% in section B–2/99, and 15.3 wt.% in section B–1/96). The upper zones are apparently depleted in comparison with the lower ones, indicating that Fe might have been leached from the top of the weathering profile (Fig. 8). However, the lack of a statistically significant difference in comparisons of the mean concentrations of Fe between samples collected from the top and bottom of the sections does not support this hypothesis.

Relatively high proportions of Fe in the water-soluble fraction were found in the *melanterite* and *intermediate zones* (up to 15.7% in section B–2/99 and 14% for B–2/99), but these are low in other zones (Table 2). Overall, the proportions of Fe in exchangeable and carbonate fractions are low, indicating that the sorption of Fe on clay minerals and the precipitation of Fe carbonates do not play a dominant role in the behavior of Fe in the Berikul waste (Fig. 8).

Iron extracted from jarosite and amorphous ferric sulfo-arsenates in the reducible fraction appears to be concentrated within the *jarosite zone* (Table 2, Fig. 8). In section B–2/99, a local high level of Fe in the reducible fraction at the *hardpan–melanterite zone* interface (samples B–2/6 and B–2/7) is just above the region where the carbonate content is above the detection limit (Tables 1, 2). A similar relationship between the position of the local maximum of Fe in the reducible fraction (sample BK–5) and an increase in the carbonate content between samples BK–5 and BK–6 can be seen in section B–1/69. Precipitation of ferric phases could result from an increase in the pH of the pore solution

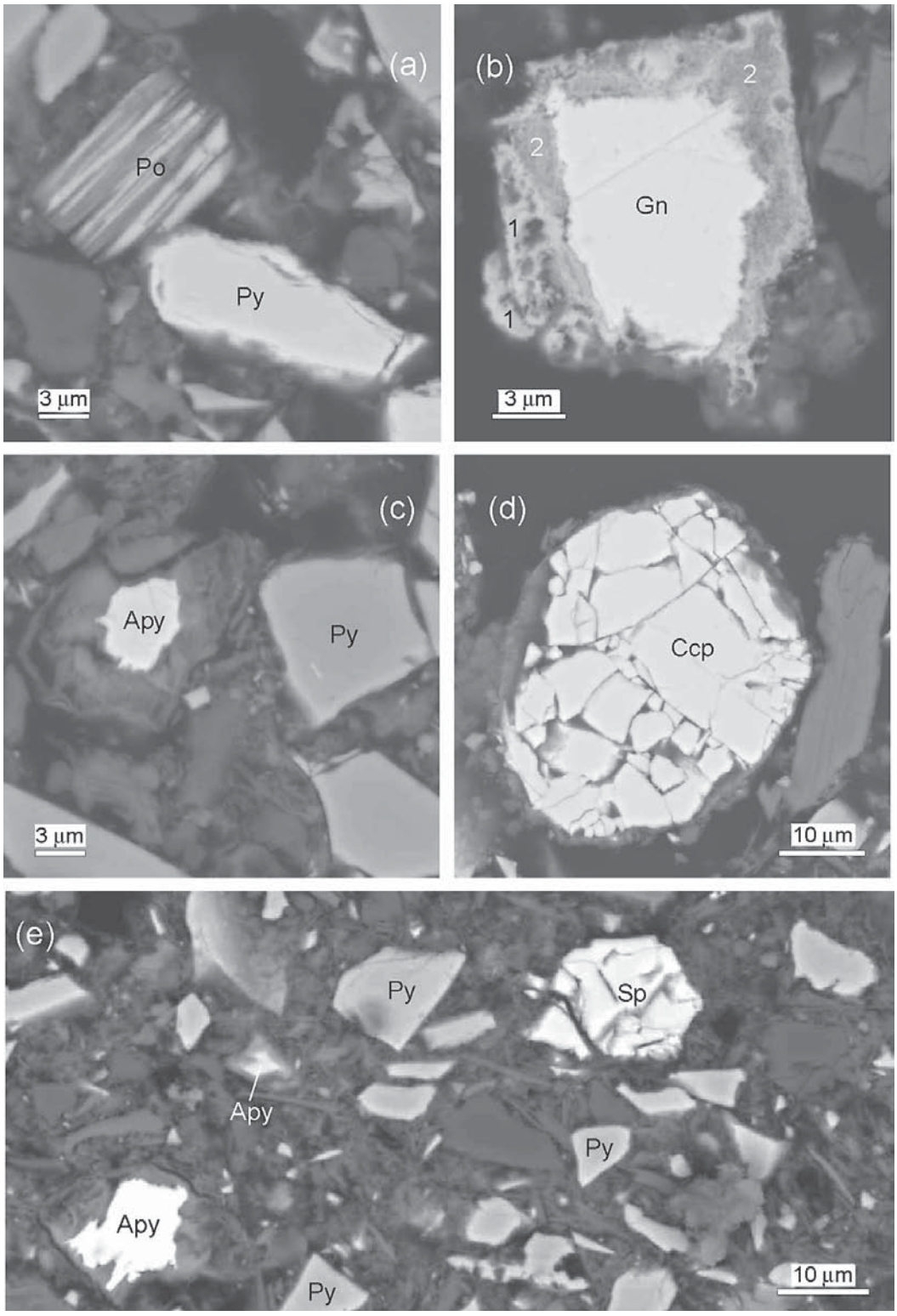
(a)
Po
Py
3 µm
(b)
2
2
Gn
1
1
3 µm
(c)
Apy
Py
3 µm
(d)
Ccp
10 µm
(e)
Py
Sp
Apy
Py
Apy
Py
10 µm

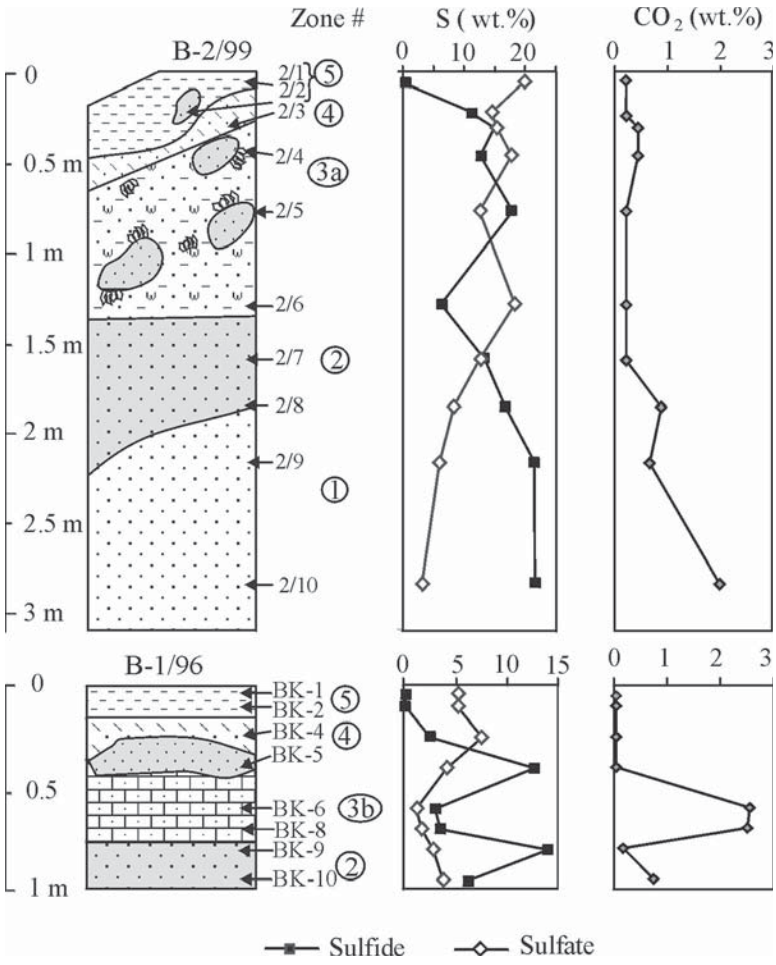

FIG. 7. Distribution of sulfur species and carbonate across sections B–2/99 and B–1/96. Zone labels are as given in Figure 4.

as it infiltrates the carbonate-buffered zone. Iron in the residual fraction is mainly bound with primary sulfides. The highest portion of this fraction (60–85% of total Fe) is found in the *slightly altered waste* and in the lithified relics. Average proportions of Fe in the residual fraction are 61% and 54%, for sections B–2/99 and B–1/96, respectively. Thus, less than about 40% of the original Fe bound to sulfides was transferred to secondary minerals.

Arsenic concentrations range from 0.02 to 5.3 wt.% (Table 3). The values decrease upward, with minimum values being in the *jarosite zone* (Fig. 8), indicating the possibility of As leaching from the upper zones and partially precipitating in the lower zones. Migration of As from the pile through the hardpan layer was also suggested by Gieré *et al*. (2003). Water-soluble, exchangeable, and carbonate fractions contain little As, being close to or below the detection limit, except within and around the *intermediate zone*, where proportions of As in the soluble fraction vary from 2.9% (B–2/3) to 10% (B–2/2) in section B–2/99. Sample BK–4, collected from the *intermediate zone* of section B–1/96, was the only one in this section with detectable As in the exchangeable fraction. Most of the As

FIG. 6. Back-scattered electron images (SEM) showing: replacement of (a) pyrrhotite, (b) galena by a zoned rim composed of (1) As–Pb–S and (2) Pb–S phases from sample 2/8, (c) arsenopyrite by iron sulfoarsenate, (d) mixture of amorphous silica and iron sulfo-arsenate surrounding chalcopyrite from sample 2/3, and (e) appearance of pyrite, sphalerite and arsenopyrite from sample 2/3.

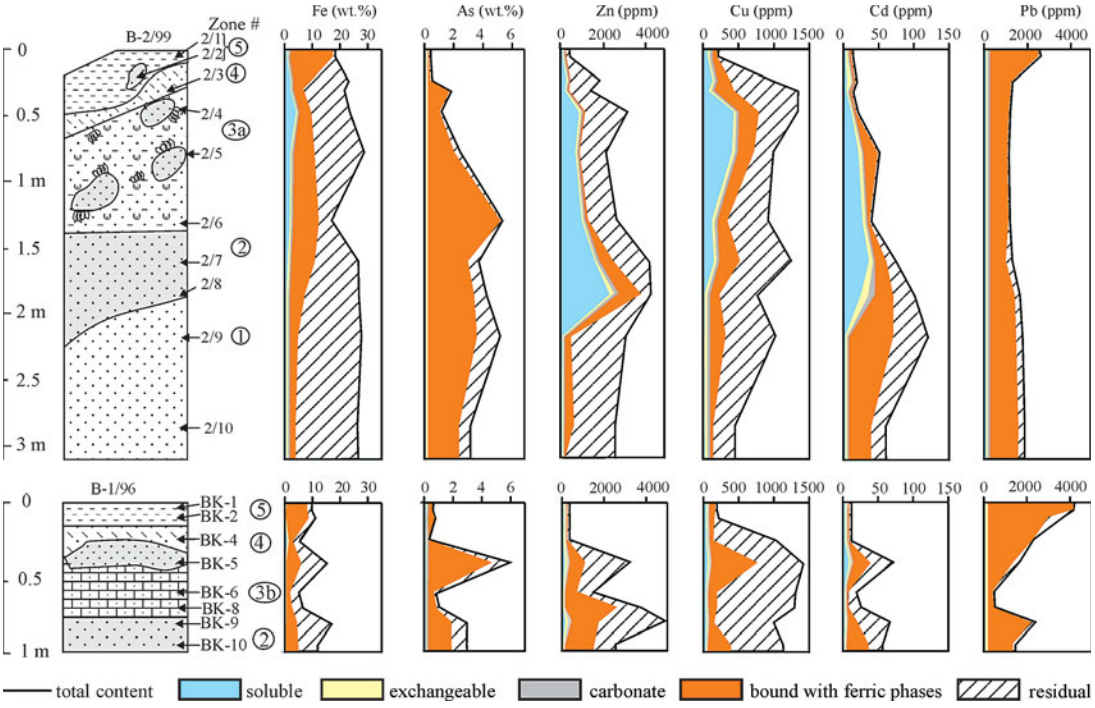

FIG. 8. Element speciation in sections B–2/99 and B–1/96 from sequential extraction. Zone labels are as given in Figure 4.

TABLE 2. Fe FRACTIONS FROM SEQUENTIAL EXTRACTION IN SECTIONS B-2/99 AND B-1/96

Zone	Sample	Soluble ppm	%	Exch. ppm	%	Carb. ppm	%	Reducible ppm	%	Residual ppm	%	Total ppm
					Section B-2/99							
5	B-2/1	0.0059	0.3	0.0034	0	0.01	0.1	16.9	94	0.9	5	17.9
4	B-2/2	1.3	5.7	0.05	0.2	0.08	0.4	8.6	37	13.0	57	23.0
	B-2/3	1.5	6.7	0.07	0.3	0.04	0.2	4.9	23	15.0	70	21.5
3a	B-2/4	3.6	15.7	0.12	0.5	0.08	0.3	6.0	26	13.0	57	22.8
	B-2/5	1.7	5.8	0.07	0.3	0.04	0.2	9.1	32	17.8	62	28.7
	B-2/6	1.1	6.3	0.09	0.5	0.06	0.3	11.3	66	4.5	27	17.0
2	B-2/7	0.54	2.0	0.08	0.3	0.04	0.2	10.0	39	15.6	59	26.3
	B-2/8	0.009	0	$<3\times10^{-4}$	0	0.005	0	7.4	27	19.4	72	26.8
1	B-2/9	$<3\times10^{-4}$	0	$<3\times10^{-4}$	0	0.003	0	4.9	18	22.9	82	27.8
	B-2/10	$<3\times10^{-4}$	0	$<3\times10^{-4}$	0	0.005	0	4.1	15	22.5	85	26.6
					Section B-1/96							
5	BK-1	$<3\times10^{-4}$	0	0.0005	<0.1	0.001	0	8.4	84	1.6	16	10.0
	BK-2	0.002	0	0.0004	<0.1	0.002	0	8.8	79	2.3	21	11.1
4	BK-4	0.79	14	0.13	2.2	0.076	1.4	1.9	34	2.7	48	5.6
	BK-5	0.017	0.1	0.009	0.1	0.027	0.2	6.0	39	9.2	60	15.3
3b	BK-6	$<3\times10^{-4}$	0	$<3\times10^{-4}$	0	0.003	0.1	1.8	36	3.2	64	5.0
	BK-8	$<3\times10^{-4}$	0	$<3\times10^{-4}$	0	0.0009	0	2.5	40	3.8	60	6.3
2	BK-9	$<3\times10^{-4}$	0	0.0015	0	0.0006	0	4.4	27	12.0	73	16.4
	BK-10	$<3\times10^{-4}$	0	$<3\times10^{-4}$	0	0.002	0	4.9	42	6.7	58	11.6

For the names of the zones, see Table 1. Exch.: Exchangeable, Carb.: Carbonates.

TABLE 3. As FRACTIONS FROM SEQUENTIAL EXTRACTION IN SECTIONS B-2/99 AND B-1/96

Zone	Sample	Soluble ppm	%	Exch. ppm	%	Carb. ppm	%	Reducible ppm	%	Residual ppm	%	Total ppm
					Section B-2/99							
5	B-2/1	<0.005	0	<0.004	0	0.004	11	0.007	22	0.01	41	0.02
	B-2/2	0.048	10.1	<0.004	0	0.036	7.3	0.29	60	0.1	22	0.4
4	B-2/3	0.055	2.9	<0.004	0	0.022	1.2	1.7	90	0.1	6	1.8
3a	B-2/4	0.056	4.8	<0.004	0	0.018	1.5	1.0	87	0.07	6	1.1
	B-2/5	<0.005	0	<0.004	0	0.029	1.2	2.0	83	0.4	15	2.4
	B-2/6	<0.005	0	<0.004	0	0.023	0.4	5.2	97	0.1	2	5.3
2	B-2/7	<0.005	0	<0.004	0	0.009	0.2	3.0	79	0.8	21	3.8
	B-2/8	<0.005	0	<0.004	0	0.01	0.2	3.4	79	0.9	21	4.3
1	B-2/9	<0.005	0	<0.004	0	0.01	0.2	3.6	70	1.5	30	5.1
	B-2/10	<0.005	0	<0.004	0	0.004	0.1	2.4	75	0.8	25	3.2
					Section B-1/96							
5	BK-1	<0.005	0	<0.004	0	0.004	1.5	0.2	91	0.01	4	0.2
	BK-2	<0.005	0	<0.004	0	0.004	0.5	0.8	94	0.04	4	0.8
4	BK-4	0.032	9.1	0.008	2.1	0.034	9.6	0.2	58	0.08	21	0.4
	BK-5	<0.005	0	<0.004	0	0.018	0.3	5.0	83	1.0	17	6.0
3b	BK-6	<0.005	0	<0.004	0	0.018	2.1	0.5	61	0.3	36	0.8
	BK-8	<0.005	0	<0.004	0	0.013	1.4	0.6	62	0.4	36	1.0
2	BK-9	<0.005	0	<0.004	0	0.013	0.5	2.0	68	0.9	31	2.9
	BK-10	<0.005	0	<0.004	0	0.022	0.8	2.0	68	0.9	31	2.9

For the names of the zones, see Table 1. Exch.: Exchangeable, Carb.: Carbonates.

is extracted, with the reducible fraction indicating an association with the ferric phases. The proportion of As in this fraction is high, even if adjusted for a systematic overestimation of 10%. The maximum As values in the reducible fraction are found just above the region where concentrations of CO_2 are above the detection limit in both cross-sections, indicating that coprecipitation of As with ferric phases may be linked to the distribution of carbonates. Arsenopyrite is the dominant form of As in the residual fraction, with the proportion decreasing upward toward the more weathered zones.

The distribution of Zn, Cu and Cd have similar features. The total concentration of Zn, Cu and Cd are lowest in the uppermost *jarosite zone*, indicating the possibility of leaching from this region (Fig. 8, Tables 4–6). The concentration of Zn and Cd increases gradually with depth to a maximum in, or just below, the *hardpan*, whereas the Cu content sharply increases in the *intermediate zone* and then decreases. Significant proportions of Zn, Cu and Cd were extracted in the soluble fraction, particularly in section B–2/99, whereas the proportions of exchangeable and carbonate fractions are negligible (Tables 4–6). The soluble forms accumulated in the center of the weathering profile, in the *melanterite zone* and in the *hardpan layer* (Fig. 8), in agreement with the mineralogical study of Sidenko *et al*. (2001), who showed melanterite from the Berikul pile to contain 0.34 wt.% Zn and 0.24 wt.% Cu. Significant quantities of Zn, Cu, and Cd in the reducible fraction of the *hardpan layer* may be related to the precipitation of Fe sulfo-arsenates and jarosite observed in the cavities (Gieré *et al*. 2003). Zinc and Cd accumulate mainly in amorphous Fe sulfo-arsenates, but Cu goes into jarosite (Sidenko *et al*. 2001, Gieré *et al*. 2003). High proportions of the residual fractions, representing primary sulfides, were found in the zones of *slightly altered waste* and in the *hardpan*.

The profile of Pb is different from that of Zn, Cu and Cd (Fig. 8, Table 7); Pb is concentrated at the top of the sections, with concentrations of <2795 and 4128 ppm in sections B–2/99 and B–1/99, respectively. This is two to three times higher than in the other zones. Most Pb was extracted in the reducible fraction. Arsenic-bearing jarosite-group minerals, the major secondary phase, contain <4.3 wt.% Pb, in contrast to <0.89 wt.% in amorphous iron sulfo-arsenate (AISA; Sidenko *et al*. 2001, Gieré *et al*. 2003), suggesting that Pb apparently accumulates in the upper zones by the precipitation of jarosite. Lead concentrations in the *melanterite zone* are lower than those in the basal section of the profile, showing that Pb has been partially leached. Lead may be mobile under the conditions of the *melanterite zone*, where Fe is divalent and not precipitated as jarosite. Lead can then migrate downward and coprecipitate

TABLE 4. Zn FRACTIONS FROM SEQUENTIAL EXTRACTION IN SECTIONS B-2/99 AND B-1/96

Zone	Sample	Soluble ppm	Soluble %	Exch. ppm	Exch. %	Carb. ppm	Carb. %	Reducible ppm	Reducible %	Residual ppm	Residual %	Total ppm
					Section B-2/99							
5	B-2/1	16	17	3	3	5	6	53	57	16	17	93
4	B-2/2	170	34	12	2	36	7	195	39	84	17	497
	B-2/3	170	54	16	5	6	2	82	25	45	14	319
3a	B-2/4	960	82	44	4	24	2	100	9	36	3	1164
	B-2/5	650	66	36	4	9	1	210	22	80	8	985
	B-2/6	1000	76	130	10	28	2	120	9	36	3	1314
2	B-2/7	1600	49	220	7	43	1	640	20	750	23	3253
	B-2/8	2300	44	230	4	280	5	1000	19	1400	27	5210
1	B-2/9	14	0.6	4	0.1	73	3	460	19	1900	78	2451
	B-2/10	<0.2	0	3	0.1	37	1	1600	61	940	37	2580
					Section B-1/96							
5	BK-1	0.8	0.6	4.5	3.6	6.0	5	87	69	28	22	126
	BK-2	3.9	2	4.4	1.9	5.8	3	170	74	47	20	231
4	BK-4	110	48	30	13	0.4	0.2	60	25	34	14	234
	BK-5	260	8	45	1.4	39	1	760	23	2100	66	3204
3b	BK-6	0	0	0.3	<0.1	36	3	680	48	690	49	1406
	BK-8	0.4	0	0.9	<0.1	180	5	2500	69	960	26	3641
2	BK-9	130	3	76	1.6	240	5	1400	28	3100	63	4946
	BK-10	0.6	0	0.6	<0.1	46	2	1440	57	1000	41	2487

For the names of the zones, see Table 1. Exch.: Exchangeable, Carb.: Carbonates.

TABLE 5. Cu FRACTIONS FROM SEQUENTIAL EXTRACTION IN SECTIONS B-2/99 AND B-1/96

Zone	Sample	Soluble ppm	Soluble %	Exch. ppm	Exch. %	Carb. ppm	Carb. %	Reducible ppm	Reducible %	Residual ppm	Residual %	Total ppm
					Section B-2/99							
5	B-2/1	81	40	6	2.9	2.5	1.2	95	46	20	10	205
	B-2/2	150	15	11	1.2	3.0	0.3	225	23	580	60	969
4	B-2/3	100	8	12	0.9	1.8	0.1	320	24	900	67	1334
3a	B-2/4	460	34	24	1.8	1.8	0.1	300	22	560	42	1346
	B-2/5	440	44	24	2.4	1.4	0.1	260	26	290	28	1015
	B-2/6	160	17	19	2.1	1.8	0.2	165	18	580	63	926
2	B-2/7	180	15	27	2.2	2.0	0.2	320	26	710	57	1239
	B-2/8	1.3	0.2	<0.3	0	2.1	0.3	230	30	530	69	763
1	B-2/9	0.6	<0.1	<0.3	0	3.2	0.3	320	31	670	68	994
	B-2/10	0.6	0.1	<0.3	0	1.5	0.3	150	32	310	68	462
					Section B-1/96							
5	BK-1	0.6	0.3	0.4	0.2	1.8	1	160	91	14	8	177
	BK-2	2.3	1	0.4	0.2	1.9	0.9	160	76	47	22	212
4	BK-4	60	6	12	1	1.8	0.2	72	7	880	86	1026
	BK-5	77	5	23	2	15	1	670	47	630	45	1415
3b	BK-6	<0.3	0	<0.3	0	3.3	0.3	190	15	1100	85	1293
	BK-8	<0.3	0	<0.3	0	4.1	0.3	190	15	1100	85	1294
2	BK-9	<0.3	0	<0.3	0	5.7	0.6	140	14	850	85	996
	BK-10	<0.3	0	<0.3	0	3.4	0.3	390	34	740	65	1133

For the names of the zones, see Table 1. Exch.: Exchangeable, Carb.: Carbonates.

with minerals of the jarosite group and AISA within the *hardpan layer*, causing higher concentrations of Pb in the reducible fraction there. The average proportion of Pb in the residual fraction of galena is only about 8% (Table 7). Two minor phases of Pb were found in zoned rims around galena (Fig. 6b). SEM–EDS analyses show the inner rim to consist of Pb and S, and the outer one, to consist of Pb, As and S. As the S*K*α peak overlaps Pb*K*α on the EDS spectra, the presence of sulfur in the rim is problematic. The inner rim could be anglesite, which is a common product of oxidation of galena in mine waste (Jambor 1994). The outer rim of Pb arsenate or sulfo-arsenate may have formed by the reaction of anglesite with As-rich solutions. These minor phases should have little effect on Pb distribution in the waste.

Mineralogical Zoning

We have calculated the weight percent of Fe phases in these weathered mine-wastes using the results of sequential extractions and bulk-chemical analyses, as well as conventional powder XRD and electron-microprobe analysis of secondary phases reported previously (Sidenko 2001, Gieré *et al*. 2003). The major phases of Fe are pyrite, arsenopyrite, melanterite, jarosite and amorphous Fe sulfo-arsenates. The proportion of major Fe phases for section B–2/99 was calculated sequentially according to the scheme presented in Table 8. Ideal formulae were assumed for pyrite, arsenopyrite, and melanterite, with the average concentration of As and Fe in jarosite and AISA being calculated from results of electron-microprobe analyses (Table 9).

The weight percent of arsenopyrite was calculated by assuming all As in the residual fraction to be in arsenopyrite (Table 8). The concentration of Fe in arsenopyrite was subtracted from total Fe in the residual fraction to obtain the weight percent of pyrite. The proportion of melanterite was estimated on the basis of Fe in the soluble fraction of the extraction. The content of AISA was calculated from the As concentration in the reducible fraction by assuming that AISA was the sole As-bearing phase extracted into the reducible fraction. This assumption is acceptable because the average concentration of As in AISA is forty times higher than in jarosite, which is dissolved at the same step of the sequential extraction. The weight percent of jarosite was determined as the difference between Fe in the reducible fraction and in AISA. This last value was calculated from the weight percent AISA, multiplied by the average Fe concentration in AISA (Table 9), divided by 100.

The distribution of primary sulfides, calculated over the weathering profile, shows a tendency for pyrite and arsenopyrite to decrease upward (Table 10). Amorphous

TABLE 6. Cd FRACTION FROM SEQUENTIAL EXTRACTION IN SECTIONS B-2/99 AND B-1/96

Zone	Sample	Soluble ppm	Soluble %	Exch. ppm	Exch. %	Carb. ppm	Carb. %	Reducible ppm	Reducible %	Residual ppm	Residual %	Total ppm
					Section B-2/99							
5	B-2/1	7.1	89	<0.2	2	0.1	2	0.6	7	<0.02	<0.2	8
	B-2/2	5.6	32	0.5	3	7.4	42	2.7	15	1.6	9	18
4	B-2/3	4.1	72	0.4	7	0.3	5	0.9	15	<0.02	<0.3	6
3a	B-2/4	10	79	0.8	6	0.5	4	1.5	12	<0.02	<0.2	13
	B-2/5	23	44	3.8	7	0.3	0.5	24	46	1.3	3	52
	B-2/6	28	74	4.5	12	2.1	6	3.0	8	<0.02	<0.1	38
2	B-2/7	37	50	6.7	9	2.7	4	16	22	12	16	74
	B-2/8	26	26	8.5	8	9.9	10	25	25	32	31	101
1	B-2/9	<0.2	0	<0.2	0	1.5	1	70	58	48	40	120
	B-2/10	<0.2	0	<0.2	0	0.7	1	38	63	22	35	61
					Section B-1/96							
5	BK-1	0.4	25	<0.2	<0.1	<0.2	0	1.2	75	<0.02	0	1.6
	BK-2	0.4	21	<0.2	<0.1	<0.2	0	1.5	79	<0.02	0	1.9
4	BK-4	3.0	73	0.9	22	<0.2	0	<0.2	0	0.2	5	4.1
	BK-5	9.7	13	2.6	4	3.3	5	25	35	32	44	34.7
3b	BK-6	<0.2	0	<0.2	0	0.6	3	6	31	13	66	19.6
	BK-8	<0.2	0	<0.2	0	1.0	4	7	27	17	69	25
2	BK-9	<0.2	0	2.8	4	3.6	5	14	22	46	69	66.4
	BK-10	<0.2	0	0.4	0.8	3.0	5	33	58	20	35	56

For the names of the zones, see Table 1. Exch.: Exchangeable, Carb.: Carbonates.

TABLE 7. Pb FRACTION FROM SEQUENTIAL EXTRACTION IN SECTIONS B-2/99 AND B-1/96

Zone	Sample	Soluble ppm	Soluble %	Exch. ppm	Exch. %	Carb. ppm	Carb. %	Reducible ppm	Reducible %	Residual ppm	Residual %	Total ppm
						Section B-2/99						
5	B-2/1	<1	0	16	1	31	1	2700	97	48	2	2795
	B-2/2	<1	0	18	1	33	2	1350	85	180	11	1581
4	B-2/3	<1	0	15	1	32	2	1300	92	66	5	1413
3a	B-2/4	<1	0	13	1	36	3	1200	93	42	3	1291
	B-2/5	<1	0	20	2	30	2	1100	86	130	10	1280
	B-2/6	<1	0	21	1	33	2	1200	80	240	16	1494
2	B-2/7	<1	0	25	2	29	2	1000	72	350	24	1404
	B-2/8	<1	0	14	1	44	3	1500	92	75	5	1633
1	B-2/9	<1	0	25	1	39	2	1600	90	120	7	1784
	B-2/10	<1	0	19	1	50	3	1700	94	45	3	1814
						Section B-1/96						
5	BK-1	10	0.2	16	0.4	42	1	3900	94	160	4	4128
	BK-2	9.7	0.3	16	0.4	36	1	2900	80	680	19	3642
4	BK-4	<1	0	6.6	0.3	<1	0	2200	98	38	2	2245
	BK-5	<1	0	8.3	0.5	2.0	0.1	1300	80	320	20	1630
3b	BK-6	<1	0	0	0.1	3.1	0.8	390	96	10	3	403
	BK-8	<1	0	0	0.1	3.2	0.7	470	98	7	2	480
2	BK-9	<1	0	1.5	0.1	21	0.9	2300	96	62	3	2385
	BK-10	<1	0	0.2	<0.1	<1	0	1200	89	140	11	1340

For the names of the zones, see Table 1. Exch.: Exchangeable, Carb.: Carbonates.

Fe sulfo-arsenate accumulates in the *slightly altered waste zone*, the *hardpan,* and reaches a maximum value of 22.9 wt.% at the base of the *melanterite zone*. This decrease may be due to dissolution of this phase in the upper layers. The melanterite content increases upward from 2.8 wt.% in upper part of the *hardpan* to 18.5 wt.% in the *melanterite zone*, and then decreases again. Jarosite increases upward to reach 18.8 wt.%, at the boundary between the *hardpan* and *melanterite zones*, and 50.4 wt.% in the uppermost *jarosite zone*.

Geochemical Processes

One of the parameters controlling the rate of metal leaching is the resistance of a specific sulfide mineral to oxidation. Mineralogical observations show that pyrrhotite and galena are generally replaced by secondary minerals, in contrast to arsenopyrite, sphalerite, chalcopyrite and pyrite (Figs. 6a, b). However, arsenopyrite appears to be less stable than pyrite, chalcopyrite and sphalerite (Figs. 6c, d). Therefore, the sequence of apparent reactivity is pyrrhotite ≈ galena > arsenopyrite > pyrite ≈ sphalerite ≈ chalcopyrite. One problem with visually estimating the relative amount of alteration of sulfide minerals is that the products of oxidation can accumulate around a grain of one sulfide (*e.g.*, anglesite rim around galena) or be transported from the surface of a different sulfide (*e.g.*, pyrite). Replacement of chalcopyrite and sphalerite are rarely observed, even in highly oxidized material (Figs. 5d, 6d, e), but the accumulation of S, As, Zn, and Cu in pore solutions indicates the dissolution of these minerals. Therefore, a grain of sulfide that shows replacement textures can appear more altered than a grain of sulfide of a similar size that has been partially dissolved. Secondly, there can be a difference in the degree of oxidation for adjacent grains of the same mineral. For example, the pyrrhotite grains shown in Figure 5c represent differing degrees of oxidation, from slightly to completely altered. Therefore, the comparison of appearance of sulfide grains from microscopic observations is limited in determining their relative reactivity. Additional methods, such sequential extraction, should be used to corroborate mineralogical results.

The average proportions of Fe, As, Zn, Cu, and Pb extracted in separate fractions after sequential analysis are given in Table 11, where the residual fraction represents mainly unoxidized sulfides. The proportion of each metal remaining in the residual fraction can provide an indication of the relative reactivity of the host sulfide in the environment of the Berikul waste. The order of decreasing metal proportions in the residual fraction is similar for both cross-sections, except for the positions of Fe and Cu. The sequence Pb < As < Zn < Cu ≈ Fe in the residual fraction assumes the sequence of sulfide reactivity to be galena > arsenopyrite > sphalerite > pyrite ≈ chalcopyrite. This is in agreement with the degree of alteration of these sulfides. Pyrrhotite was not included in this sequence because it is a minor phase.

Using geochemical characterization, we define three major regions within the profile representing different stages of weathering of the high-sulfide waste. The basal region, consisting of *slightly altered sulfide waste* and the *hardpan layer*, is characterized by the presence

TABLE 8. A SCHEME FOR THE CALCULATION OF WEIGHT PERCENTAGE OF THE PHASES

Phase	Formulae
Arsenopyrite	$Q_{Apy} = C\,As_{Residual} \times M_{FeAsS} / M_{As}$
Pyrite	$Q_{Py} = (C\,Fe_{Residual} - Q_{Apy} \times M_{Fe} / M_{FeAsS}) \times M_{FeS2} / M_{Fe}$
Melanterite	$Q_{Mln} = C\,Fe_{Soluble} \times M_{FeSO4\cdot7H2O} / M_{Fe}$
AISA	$Q_{AISA} = C\,As_{Reducible} / C\,As_{AISA} / 100\%$
Jarosite	$Q_{Jrs} = (C\,Fe_{Reducible} - Q_{AISA} \times C\,Fe_{AISA}/100\%) \times M_{KFe3(SO4)2(OH)6} / M_{Fe}$

Note: Q_{Phase} is the wt.% of the phase, $C\,El_{fraction/phase}$ is the concentration of element El in a fraction or in a phase (wt.%), $M_{Phase/El}$ is the molar weight of a phase or an element (g/M). Symbols: Apy: arsenopyrite, Py: pyrite, Mln: melanterite, AISA: amorphous iron sulfo-arsenate, Jrs: jarosite.

TABLE 9. CHEMICAL COMPOSITION OF AMORPHOUS IRON SULFO-ARSENATES (AISA) AND JAROSITE

Element	AISA, *n* = 184		Jarosite, *n* = 46	
	Ave.	St. dev.	Ave.	St. dev.
Al wt.%	1.58	1.05	0.12	0.10
As	22.74	6.25	0.66	0.53
Ca	0.04	0.03	0.04	0.02
Cu	0.07	0.06	0.07	0.10
Fe	31.58	6.25	28.14	2.21
K	0.06	0.88	1.85	0.77
Na	-	-	0.45	0.01
Pb	0.46	0.80	1.16	1.62
S	7.60	1.55	11.36	0.91
Si	0.66	0.61	0.17	0.24
Zn	0.28	0.15	0.05	0.07

Modified after Gieré *et al*. (2003).

TABLE 10. CALCULATED WEIGHT PERCENTAGE OF MAJOR Fe PHASES IN SECTION B-2/99

Z	S	D	Apy	Py	Mln	AISA	Jrs
5	B-2/1	5	0.03 ± 0.02	1.81 ± 0.2	0.30 ± 0.04	0.03 ± 0.01	50.4 ± 6.1
5	B-2/2	23	0.3 ± 0.2	25.7 ± 3.3	6.8 ± 0.8	1.26 ± 0.39	24.4 ± 3.5
4	B-2/3	30	0.3 ± 0.2	29.8 ± 3.8	7.4 ± 0.9	7.4 ± 2.3	7.8 ± 4.4
3a	B-2/4	45	0.2 ± 0.1	25.7 ± 3.2	18.5 ± 2.2	4.5 ± 1.4	13.7 ± 3.8
3a	B-2/5	75	0.9 ± 0.6	34.8 ± 4.8	8.6 ± 1.0	9.0 ± 2.7	18.8 ± 6.5
3a	B-2/6	125	0.3 ± 0.2	8.9 ± 1.3	5.5 ± 0.7	22.9 ± 7.0	12.0 ± 12.2
2	B-2/7	155	1.9 ± 1.3	30.1 ± 4.9	2.8 ± 0.3	13.1 ± 4.0	18.8 ± 8.4
2	B-2/8	180	2.2 ± 1.5	37.5 ± 6.0	0	14.9 ± 4.6	7.9 ± 8.0
1	B-2/9	210	3.8 ± 2.6	43.9 ± 7.9	0	15.9 ± 4.9	0
1	B-2/10	275	1.9 ± 1.3	43.7 ± 6.6	0	10.4 ± 3.2	2.5 ± 5.2

Symbols: Apy: arsenopyrite, Py: pyrite, Mln: melanterite, AISA: amorphous iron sulfo-arsenate, Jrs: jarosite. Note: the names of the zones (Z) are presented in Table 1. S: Sample numbers; depth D in cm.

of both acid-producing sulfides and acid-consuming carbonates. The middle portion including the *melanterite* and *intermediate zones*, contains only acid-producing sulfides, whereas in the uppermost region, neither carbonates nor sulfides are present.

During the first stage, the acid produced by the oxidation of sulfides (reaction 1) can be neutralized by the dissolution of dolomite (reaction 2) at the base of the *hardpan layer*.

$$FeAsS + 1.5\ H_2O + 3.25\ O_2(aq) \rightarrow 2\ H^+ + SO_4^{2-} + HAsO_4^{2-} + Fe^{2+} \quad (1)$$

$$CaMg(CO_3)_2 + 4\ H^+ + SO_4^{2-} \rightarrow CaSO_4{\bullet}2H_2O + Mg^{2+} + 2\ CO_{2(g)} \quad (2)$$

The gypsum framework in the *hardpan layer* is formed as a result of these reactions. Therefore, the *hardpan* forms at the upper boundary of the carbonate-buffered zone, where acidic water percolating downward reacts with carbonates. In the *slightly altered sulfide waste*, Fe, As, Pb, Zn, Cd, and Cu accumulate in the reducible fraction that represents the ferric phases, jarosite and Fe sulfo-arsenates. Ferric iron, produced by the oxidation of Fe^{2+} (equation 3), results in the precipitation of jarosite (equation 4) and Fe sulfo-arsenates (equation 5). The formula of bukovskýite is used in equation 5 as it is the mineral closest in composition to the AISA in Berikul waste (Gieré *et al*. 2003).

$$2\ Fe^{2+} + 0.5\ O_2 + 2\ H^+ \rightarrow Fe^{3+} + H_2O \quad (3)$$

$$K^+ + Fe^{3+} + 2\ SO_4^{2-} + 6\ H_2O \rightarrow KFe^{3+}(SO_4)_2(OH)_6 + 6\ H^+ \quad (4)$$

$$2\ Fe^{3+} + HAsO_4^{2-} + SO_4^{2-} + 8\ H_2O \rightarrow Fe^{3+}{}_2(AsO_4)(SO_4)(OH){\bullet}7H_2O\ \text{(bukovskýite)} + 2H^+ \quad (5)$$

Protons on the right of reactions (4) and (5) are consumed by the dissolution of carbonate (reaction 2), resulting in reactions (4) and (5) shifting to the right according Le Chatelier's principle. In this way, carbonate dissolution promotes the precipitation of ferric phases. The overall reaction of carbonate dissolution and the precipitation of Fe sulfo-arsenates can be expressed as:

$$MgCa(CO_3)_2 + 2\ Fe^{3+} + HAsO_4^{2-} + SO_4^{2-} + 8\ H_2O \rightarrow Fe^{3+}{}_2(AsO_4)(SO_4)(OH){\bullet}7H_2O + Ca^{2+} + Mg^{2+} + 2\ HCO_3^- \quad (6)$$

During the second stage, acid generated in the *hardpan* and upper regions completely dissolves the carbonates, and the pH of the pore solution decreases to 1.7 (Gieré *et al*. 2003), controlling the second stage of weathering observed in the *melanterite* and *intermediate zones*. With increasing acidity, the reactions (4) and (5) move to the left, leading to dissolution of the ferric phases in the central region. The dissolution of the Fe sulfo-arsenates is inferred by their decrease from sample B–2/6 (B–2/99) upward (Table 10). This releases As, Pb, Zn, Cd and Cu back into solution, producing the high concentrations found in pore waters from the *melanterite* and *intermediate zones*. Jarosite remains constant in these zones, indicating that it is more stable than the Fe sulfo-arsenates. The rate of Fe^{2+} oxidation (reaction 3) in acidic water is limited even if the reaction is bacterially catalyzed (Singer & Stumm 1970). Under these conditions, Fe^{3+} produced by reaction (3) is utilized by sulfide oxidation (reaction 7):

$$FeS_2\ \text{(pyrite)} + 14\ Fe^{3+} + 8\ H_2O \rightarrow 15\ Fe^{2+} + 16\ H^+ + 2\ SO_4^{2-} \quad (7)$$

The order of reaction rates from the experimental oxidation of sulfides by Fe^{3+} at pH 2 (Wiersma & Rimstidt 1984, Rimstidt *et al*. 1994) agrees with the sequence of sulfide reactivity in the Berikul mine-wastes, indicating that Fe^{3+} is the principal oxidant of the sulfides. If reaction (7) is sufficient to consume all the Fe^{3+} produced by reaction (3), Fe^{2+} and SO_4^{2-} will accumulate in solution, and melanterite will precipitate (reaction 8):

$$Fe^{2+} + SO_4^{2-} + 7\ H_2O \rightarrow Fe^{2+}SO_4{\bullet}7H_2O\ \text{(melanterite)} \quad (8)$$

The saturation indices of melanterite, calculated from the compositions of water, agree with the mineralogical results (Sidenko *et al*. 2001). In the central carbonate-free region, significant portions of Zn, Cu and Cd coprecipitate with melanterite. Copper and zinc can substitute for Fe^{2+} in melanterite owing to the similarity of the melanterite, zincmelanterite, and boothite structures (Jambor *et al*. 2000).

The third stage begins with a continued decrease of sulfides due to progressive oxidation in the upper region. The concentration of oxygen increases rapidly toward the surface within the upper 0.5 m of the sulfide tailings (Blowes *et al*. 1991). This increase results in a higher production of Fe^{3+} in solution (reaction 3),

TABLE 11. AVERAGE PERCENTAGE OF ELEMENTS IN SEPARATE FRACTIONS FROM SEQUENTIAL EXTRACTIONS FOR SECTIONS B-2/99 AND B-1/96

Element	Soluble		Exchangeable		Carbonates		Reducible		Residual	
	B-2/99	B-1/96	B-2/99	B-1/96	B-2/99	B-1/96	B-2/99	B-1/96	B-2/99	B-1/96
Fe wt.%	4.9	2.0	0.2	0.3	0.2	0.2	34.0	43.0	61.0	54.0
As	2.3	1.7	0.9	0.6	1.4	2.2	77.2	70.9	18.1	24.6
Zn	42.8	9.0	3.7	2.7	2.4	2.7	26.1	46.0	23.3	39.6
Pb	0.1	0.1	1.2	0.2	2.4	0.5	88.1	91.4	8.3	7.8
Cu	16.7	1.8	1.3	0.5	0.3	0.5	27.5	31.2	54.1	65.9
Cd	44.5	15.4	5.2	5.6	3.9	4.5	30.5	34.6	15.9	39.9

Note: averages were weighted according to the interval thickness represented by individual samples.

which causes sulfides to oxidize rapidly (reaction 7), decreasing the sulfide content in the solid waste upward from the intermediate zone (Fig. 7). The loss of sulfides results in a further accumulation of Fe^{3+} in solution, which can no longer be consumed by the sulfides (reaction 7). This accumulation results in the precipitation of ferric phases such as the *jarosite zone* (reaction 4), where a decrease in sulfide can be correlated with an increase in Fe in the reducible fraction.

Lead can substitute for K in jarosite, resulting in a jarosite–plumbojarosite solid solution, whereas substitutions of Zn, Cu and Cd are limited to less than 2 wt.% (Dutrizac & Jambor 2000). This fact explains values of up to 4.3 wt.% of Pb in jarosite from the Berikul waste with maximum contents of Cu of 0.24 wt.% and of Zn of <0.17 wt.% (Sidenko *et al*. 2001, Gieré *et al*. 2003). If the mass of As contained in AISA and jarosite is calculated from Table 9 and 10, it can be seen that only about 10% of the As leached from ASIA can be attenuated by jarosite. Thus, Pb accumulates in the uppermost *jarosite zone*, whereas As, Zn, Cu and Cd have been mostly removed (Fig. 8) by the dissolution of primary minerals and of previously formed sulfoarsenates and melanterite during the advancement of the weathering front.

The equilibrium between jarosite and melanterite, which depends on pH and redox conditions (reaction 9), controls whether metals coprecipitate with water-soluble melanterite or with a more stable phase such as jarosite:

$$6\ Fe^{2+}SO_4{\bullet}7H_2O + 1.5\ O_2 + 2\ K^+ \rightarrow 2\ KFe^{3+}{}_3\ (SO_4)_2(OH)_6 + 2\ SO_4^{2-} + 33\ H_2O + 6\ H^+ \quad (9)$$

Jarosite and melanterite are common products of pyrite oxidation observed in mine waste and oxidized sulfide ores (Jambor 1994), but the occurrence of a ferrous sulfate (melanterite) zone between zones containing ferric phases (*i.e*., jarosite) is an unusual feature. Logically, melanterite should be converted to jarosite during progressive oxidation (Jambor *et al*. 2000), but we found 18.8 wt.% of jarosite below the *melanterite zone* in the upper part of the hardpan (Table 10). A diagram was constructed to show the equilibrium between melanterite and jarosite at different values of pH and redox conditions in the system S–O–H–Fe–K at 25ºC (Fig. 9). We used the thermodynamic database constructed for this system by Alpers *et al*. (1989) and activities obtained from the average concentrations of K and SO_4^{2-} in pore water previously determined for the Berikul waste (Gieré *et al*. 2003). The measured pH of the pore water was plotted against oxygen fugacity calculated from Eh values obtained in previous studies (Sidenko *et al*. 2001). The points form a trend, which crosses the jarosite–melanterite equilibrium boundary parallel to the pH axis under the conditions of low fugacity of oxygen, owing to acidification following complete carbonate dissolution in the upper part of the *hardpan layer.* Melanterite is stable under the acidic and relatively reducing conditions of the pore waters squeezed from the *melanterite zone* (Fig. 9). The equilibrium boundary is then crossed vertically, as oxygen fugacity increases owing to diffusion from the surface and to the decrease in sulfide oxidation that consumed oxygen and Fe^{3+} (reaction 1). Therefore, jarosite becomes stable in and above the *intermediate zone* (Fig. 9), where conditions are more oxidizing than in the *melanterite zone*. Thus, the precipitation of melanterite or jarosite depends on the sulfide content controlling redox conditions and on the presence of carbonates buffering pH.

Conclusions

Three stages of weathering can be distinguished at the Berikul high-sulfide waste pile. During an early stage, acid produced by sulfide oxidation is neutralized by carbonate dissolution, causing the formation of a cemented layer and coprecipitation of metals and arsenic with ferric phases such as amorphous Fe sulfoarsenates. The next stage begins after the complete dissolution of carbonates, when the acid generated cannot be neutralized. During this stage, ferric sulfoarsenates dissolve, releasing arsenic and metals to the solution. At a low pH, the rate of metal leaching from the waste is determined by the reaction rate of sulfides with ferric ion. This reaction produces ferrous Fe, sulfate and metals in the pore water, resulting in the precipitation of Zn-, Cu-, and Cd-bearing melanterite. This stage ends with the almost complete oxidation of sulfides. As a result, Fe^{3+} that has been consumed previously by sulfide oxidation accumulates in the solution,

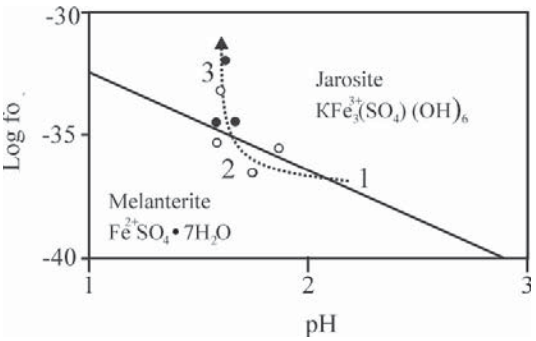

FIG. 9. Solid phase equilibria in the system S–O–H–Fe–K at T = 25°C, log *a* K^+ = –4.0, log *a* SO_4^{2-} = 0.3. Circles show the composition of pore solutions squeezed from samples of the *intermediate* (solid circles) and *melanterite zones* (open circles). The trend line and numbers show the evolution of log $f(O_2)$ – pH conditions during weathering. The numbers show possible log $f(O_2)$ and pH conditions during first (1), second (2) and third (3) stages of weathering.

and Pb-containing jarosite precipitates. By this stage, significant proportions of As, Zn, Cu and Cd have been leached from the ore residue by acidic solutions.

The acid generation in Berikul mine-waste could be controlled by placing a clay and silt cover to prevent oxygen diffusion and infiltration of oxygenated water. Building a rock berm is also recommended, as it would prevent erosion of the slopes and surface runoff.

Acknowledgements

This study was supported by "Stadinost" grant of the United Institute of Geology, Geophysics and Mineralogy (Novosibirsk, Russia) and an NSERC Discovery grant to B.L. Sherriff. We thank the two anonymous reviewers, Drs. G.S. Clark, D. Paktunc and R.F. Martin for helpful comments on the manuscript.

References

Alpers, C.N., Nordstrom, D.K. & Ball, J.E. (1989): Solubility of jarosite solid solutions precipitated from acid mine waters, Iron Mountain, California, USA. *Sci. Geol. Bull.* **42**, 4, 281-298.

Blowes, D.W. & Jambor, J.L. (1990): The pore-water geochemistry and the mineralogy of the vadose zone of sulfide tailings, Waite Amulet, Quebec, Canada. *Appl. Geochem.* **5**, 327-346.

_____ & Ptacek, C.J. (1994): Acid-neutralization mechanisms in inactive mine tailings. *In* Environmental Geochemistry of Sulfide Mine Wastes (J.L. Jambor & D.W. Blowes, eds.). *Mineral. Assoc. Can., Short Course Vol.* **22**, 271-292.

_____, Reardon, E.J., Jambor, J.L. & Cherry, J.A. (1991): The formation and potential importance of cemented layers in inactive sulfide mine tailings. *Geochim. Cosmochim. Acta* **55**, 965-978.

Bock, R. (1984): *A Handbook of Decomposition Methods in Analytical Chemistry.* "Khimiya". Moscow, Russia (in Russ.).

Bortnikova, S.B., Smolyakov, B.S., Sidenko, N.V., Kolonin, G.R., Bessonova, E.P. & Androsova, N.V. (2001): Geochemical consequences of acid mine drainage into a natural reservoir: inorganic precipitation and effects on plankton activity. *J. Geochem. Expl.* **74**, 127-139.

Dold, B. & Fontboté, L. (2001): Element cycling and secondary mineralogy in porphyry copper tailings as a function of climate, primary mineralogy and mineral processing. *J. Geochem. Expl.* **74**, 3-55.

Dutrizac, J.E. & Jambor, J.L. (2000): Jarosites and their application in hydrometallurgy. *In* Sulfate Minerals: Crystallography, Mineralogy and Environmental Significance (C.N. Alpers, J.L. Jambor & D.K. Nordstrom, eds.). *Rev. Mineral. Geochem.* **40**, 405-452.

Fanfani, L., Zuddas, P. & Chessa, A. (1997): Heavy metals speciation analysis as a tool for studying mine tailings weathering. *J. Geochem. Expl.* **58**, 241-248.

Gieré, R., Sidenko, N.V. & Lazareva, E.V. (2003): The role of secondary minerals in controlling the migration of arsenic and metals from high-sulfide wastes (Berikul gold mine, Siberia). *Appl. Geochem.* **18**, 1347-1359.

Jambor, J.L. (1994): Mineralogy of sulfide rich tailings and their oxidation products *In* Environmental Geochemistry of Sulfide Mine Wastes (J.L. Jambor & D.W. Blowes, eds.). *Mineral. Assoc. Can., Short Course Vol.* **22**, 59-102.

_____, Nordstrom, D.K. & Alpers, C.N. (2000): Metal-sulfate salts from sulfide mineral oxidation. *In* Sulfate Minerals: Crystallography, Mineralogy and Environmental Significance (C.N. Alpers, J.L. Jambor & D.K. Nordstrom, eds.). *Rev. Mineral. Geochem.* **40**, 303-350.

Jeffery, P.G. & Hutchison, D. (1983): *Chemical Methods of Rock Analysis* (3rd ed.). Pergamon Press, New York, N.Y.

McGregor, R.G., Blowes, D.W. & Robertson, W.D. (1995): The application of chemical extractions to sulfide tailings at the Copper Cliff tailings area, Sudbury, Ontario. Conf. on Mining and the Environment (Sudbury), 5-6 (abstr.).

Paktunc, D. (2003): mNP: a Computer Based Program to Determine Acid Generating and Neutralization Potentials of Mine Wastes Based on Mineralogical Composition. *CANMET Rep.* **MMSL 03–030(TR)**.

Ribet, I., Ptacek, C.J., Blowes, D.W. & Jambor, J.L. (1995): The potential for metal release by reductive dissolution of weathered mine tailings. *J. Contam. Hydrol.* **17**, 239-273.

Rimstidt, J.D., Chermak, J.A. & Gagen, P.M. (1994): Rates of reaction of galena, sphalerite, chalcopyrite and arsenopyrite with Fe (III) in acidic solutions. *In* Environmental Geochemistry of Sulfide Oxidation (C.N. Alpers & D.W. Blowes, eds.). *Am. Chem. Soc., Symp. Ser.* **550**, 2-13.

Sidenko, N.V. (2001): *Migration of Heavy Metals and Arsenic in Supergene Zone of Sulfide Mine Waste at the Berikul Mine*. Ph.D. thesis, Institute of Geology of Siberian Branch of Russian Academy of Sciences, Novosibirsk, Russia (in Russ.).

_____, Lazareva, E.V. & Kolmogorov, Y.P. (2001): coprecipitation of As, Zn, Cu and Pb with secondary iron minerals in the high-sulfide mine waste, Berikul mine, Russia. Tenth Symp. on Water–Rock Interaction (Sardinia), Extended Abstr., 1281-1284.

Singer, P.C. & Stumm, W. (1970): Acid mine drainage: the rate determining step. *Science* **167**, 1121-1123.

Tessier, A., Cambell, P.G.C. & Bisson, M. (1979): Sequential extraction procedure for the speciation of particulate trace metals. *Anal. Chem.* **51**, 844-850.

Wiersma, C.L. & Rimstidt, J.D. (1984): Rates of reaction pyrite and marcasite with ferric iron at pH 2. *Geochim. Cosmochim. Acta* **48**, 85-92.

Received September 11, 2003, revised manuscript accepted August 9, 2005.